

# CHEMISTRY

## A European Journal

A Journal of



### Accepted Article

**Title:** Selenocysteine as a substrate, an inhibitor and a mechanistic probe for bacterial and fungal iron-dependent sulfoxide synthases.

**Authors:** Kristina V. Goncharenko, Sebastian Flückiger, Cangsong Liao, David Lim, Anja R. Stampfli, and Florian P. Seebeck

This manuscript has been accepted after peer review and appears as an Accepted Article online prior to editing, proofing, and formal publication of the final Version of Record (VoR). This work is currently citable by using the Digital Object Identifier (DOI) given below. The VoR will be published online in Early View as soon as possible and may be different to this Accepted Article as a result of editing. Readers should obtain the VoR from the journal website shown below when it is published to ensure accuracy of information. The authors are responsible for the content of this Accepted Article.

**To be cited as:** *Chem. Eur. J.* 10.1002/chem.201903898

**Link to VoR:** <http://dx.doi.org/10.1002/chem.201903898>

Supported by  
**ACES**

WILEY-VCH

# Selenocysteine as a substrate, an inhibitor and a mechanistic probe for bacterial and fungal iron-dependent sulfoxide synthases.

Kristina V. Goncharenko<sup>1</sup>, Sebastian Flückiger<sup>1</sup>, Cangsong Liao<sup>1</sup>, David Lim<sup>1</sup>, Anja R. Stampfli<sup>1</sup>, Florian P. Seebeck<sup>1\*</sup>

<sup>1</sup> Department of Chemistry, University of Basel, Mattenstrasse 24a, Basel 4002, Switzerland

**ABSTRACT:** Sulfoxide synthases are non-heme iron enzymes that participate in the biosynthesis of thiohistidines such as ergothioneine and ovothiol A. The sulfoxide synthase EgtB from *Chloracidobacterium thermophilum* (*CthEgtB*) catalyzes oxidative coupling between the side chains of N- $\alpha$ -trimethyl histidine (TMH) and cysteine (Cys) in a reaction that entails complete reduction of molecular oxygen, carbon-sulfur (C-S) and sulfur-oxygen (S-O) bond formation and carbon-hydrogen (C-H) bond cleavage. In this report we show that bacterial sulfoxide synthases cannot efficiently turnover selenocysteine (SeCys) as an alternative substrate because the sulfur-to-selenium substitution. In contrast, the sulfoxide synthase from the filamentous fungus *Chaetomium thermophilum* (*CthEgt1*) catalyzes C-S and C-Se bond formation at almost equal efficiency. We discuss evidence suggesting that this difference emerges from different modes of oxygen-activation.

Accepted Manuscript

## INTRODUCTION

Ergothioneine (**1**, Figure 1) is a ubiquitous bacterial and fungal natural product that may also play an important role in human health. The unique redox activity of the 2-mercaptoimidazole ring suggest that **1** is likely involved in cellular redox homeostasis.<sup>[1]</sup> The quest to identify specific physiological roles of **1** has received an interesting parallel with the discovery of the selenium containing analogue selenoneine (**2**, Figure 1). This compound was discovered as the major organoselenide in marine fish.<sup>[2]</sup> Questions regarding the physiological activity of **2** are also relevant to human health because it accumulates in individuals with a seafood rich diet.<sup>[3]</sup>

One way to study functions of natural products is to examine their biosynthetic origin and the environmental conditions that make their production advantageous for individual cells or cellular communities. For example, discovery of ergothioneine biosynthetic genes in mycobacteria enabled the first definitive demonstration that this antioxidant protects *Mycobacterium tuberculosis* against oxidative stress and supports drug susceptibility and virulence.<sup>[4]</sup> Many bacteria, some archaea and most fungi produce **1** in an oxygen-dependent reaction cascade that attaches a sulfur atom to the imidazole ring of N- $\alpha$ -trimethylhistidine (TMH, Figure 1).<sup>[5]</sup> Oxidative coupling of Cys or  $\gamma$ -glutamyl cysteine ( $\gamma$ -GCys) to TMH is catalyzed by iron-dependent sulfoxide synthases in a complex reaction involving carbon-sulfur (C-S) bond formation, oxygen atom transfer to sulfur (S-O), carbon-hydrogen (C-H) bond cleavage and complete reduction of molecular oxygen (O<sub>2</sub>, Figure 1). The sequence of these elementary steps and the structure of the involved intermediates are not yet fully understood despite a number of empirical and theoretical investigations.<sup>[6]</sup> Less is known about the biosynthetic origin of **2**. Given that most enzymes involved in sulfur metabolism do not discriminate against selenium,<sup>[7]</sup> it is possible that **2** emerges from the same chemistry as **1** (Figure 1). This pathway could start with the entry of inorganic selenium into the sulfur assimilation pathway leading to production of selenocysteine (SeCys) by Cys-biosynthetic enzymes. Support for this idea comes from the demonstration that *Schizosaccharomyces pombe* grown in selenium-enriched media produces small but detectable amounts of **2** in a sulfoxide synthase-dependent manner.<sup>[8]</sup> The limited accessibility of selenoneine by fermentation or by isolation from marine fish is a major roadblock for exploring and exploitation of selenoneine as a therapeutic.<sup>[3c, 8b, 9]</sup> A strategy for chemical synthesis has been published just recently.<sup>[10]</sup>

In this report we examined the efficiency of sulfoxide synthase-catalyzed carbon-selenium (C-Se) bond formation. This study revealed that bacterial sulfoxide synthases are highly inefficient catalysts for this reaction. In contrast, the type of sulfoxide synthases that only occurs in fungi catalyzes C-Se and C-S bond formation with similar efficiency. These observations suggest that naturally occurring **2** is either exclusively produced by fungal sulfoxide synthases, or by an entirely different set of enzymes. Kinetic characterization of the sulfoxide synthase from *Chloracidobacterium thermophilum* (CthEgtB) revealed that substituting Cys with

SeCys reduces the enzymes efficiency of O<sub>2</sub> activation and introduces a primary substrate kinetic isotope effect that is obfuscated in the native reaction. These findings provide novel insight into the catalytic mechanism of sulfoxide synthases.

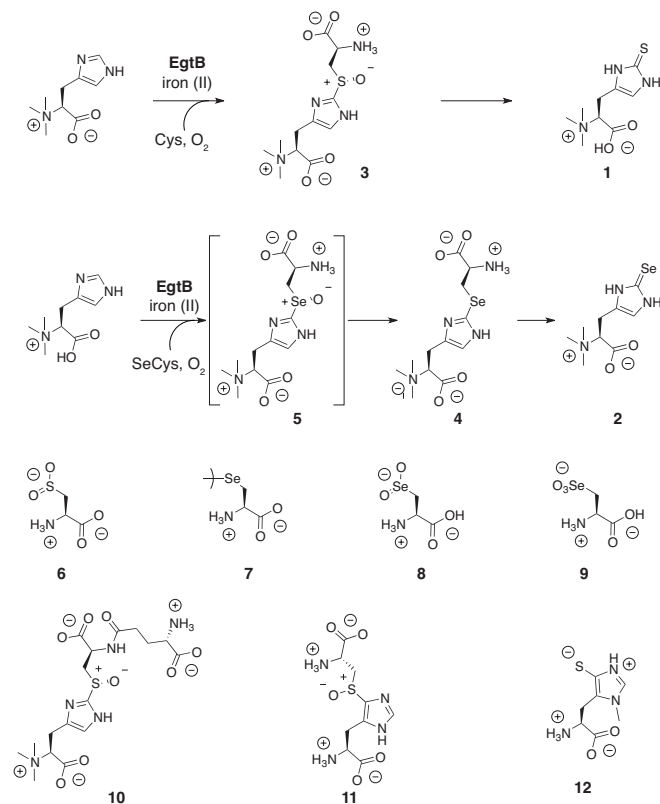


**Figure 1.** *CthEgtB* catalyzes the production of sulfoxide **3** which is converted to ergothioneine (**1**) by a PLP-dependent  $\beta$ -lyase.<sup>[5b, 6f, 11]</sup> In presence of SeCys *CthEgtB* can catalyze the formation of the selenoether **4**.<sup>[8a]</sup> Compounds **5** – **12** are discussed in the text.

## Results and Discussion

**SeCys is a poor substrate for *CthEgtB*.** We have previously described the crystal structure of *CthEgtB* and shown that this type of bacterial sulfoxide synthase accepts TMH and Cys as substrates.<sup>[6f, 12]</sup> At neutral pH and at room temperature *CthEgtB* produces sulfoxide **3** as the main product (80 %) and cysteine dioxide as a minor product (**6**, 20 %, Figure 1). Under steady-state conditions consumption of Cys is characterized by a  $k_{\text{cat}}$  of 0.14 s<sup>-1</sup> and apparent  $K_{\text{M}}$  values of 27  $\mu\text{M}$  for Cys and 65  $\mu\text{M}$  for TMH.<sup>[6f]</sup> Quantification of SeCys consumption by the same assay was complicated by the considerable reactivity of selenols towards O<sub>2</sub> and towards reducing agents. SeCys can react with O<sub>2</sub> to form the corresponding diselenide (**7**), the seleninic acid (**8**) or the selenonic acid (**9**). The latter two can undergo syn  $\beta$ -elimination causing irreversible destruction of SeCys. Oxidation to the diselenide is reversible in the presence of the reducing agent tris(2-carboxyethyl)phosphine (TCEP). Therefore, diselenide formation does not contribute to the observed consumption of SeCys. On the other hand, reductive deselenation by TCEP is also a potential avenue for irreversible destruction of SeCys.<sup>[13]</sup> Because of these possible side reactions we first needed to establish the rate of SeCys

consumption in the absence of *CthEgtB*. In a reaction containing 0.5 mM SeCys, 0.5 mM TMH, 2 mM TCEP, in a 100 mM phosphate buffer at pH 8.0 we observed SeCys consumption at an initial rate of  $4 \pm 1$   $\mu\text{M}/\text{min}$  (Figure S1). Addition of 1, 3 or 10  $\mu\text{M}$  enzyme did not increase this rate, suggesting that *CthEgtB*-catalyzed consumption of SeCys cannot be faster than  $2 \times 10^{-3} \text{ s}^{-1}$ . We also found no measurable indication that *CthEgtB* stimulates oxidation of TCEP or ascorbate (Figure S1), suggesting that enzyme-catalyzed  $\text{O}_2$  activation is at least 10-fold slower when Cys is substituted with SeCys.

Careful analysis of SeCys-containing reactions by HPLC and high-resolution electrospray ionization mass spectrometry revealed the selenoether **4** as a genuine enzyme-dependent product (HR ESI-MS:  $m/z$  obs. 409.0360, calc. 409.0362,  $\text{C}_{12}\text{H}_{19}\text{N}_4\text{O}_4\text{SeNa}_2$ , Figure S2). The same compound has been implicated as an intermediate in the biosynthesis of **2** by *S. pombe*.<sup>[8a]</sup> In the presence of 0.5 mM SeCys and 0.5 mM TMH *CthEgtB* produces **4** at a rate of  $(1.2 \pm 0.2) \times 10^{-3} \text{ s}^{-1}$  (Figure S3) which is roughly 200-fold slower than formation of sulfoxide **3** under the same conditions.<sup>[6f]</sup> We did not observe selenoxide **5** which is not surprising because selenoxides are rapidly reduced in the presence of selenols, ascorbate or TCEP.<sup>[14]</sup>

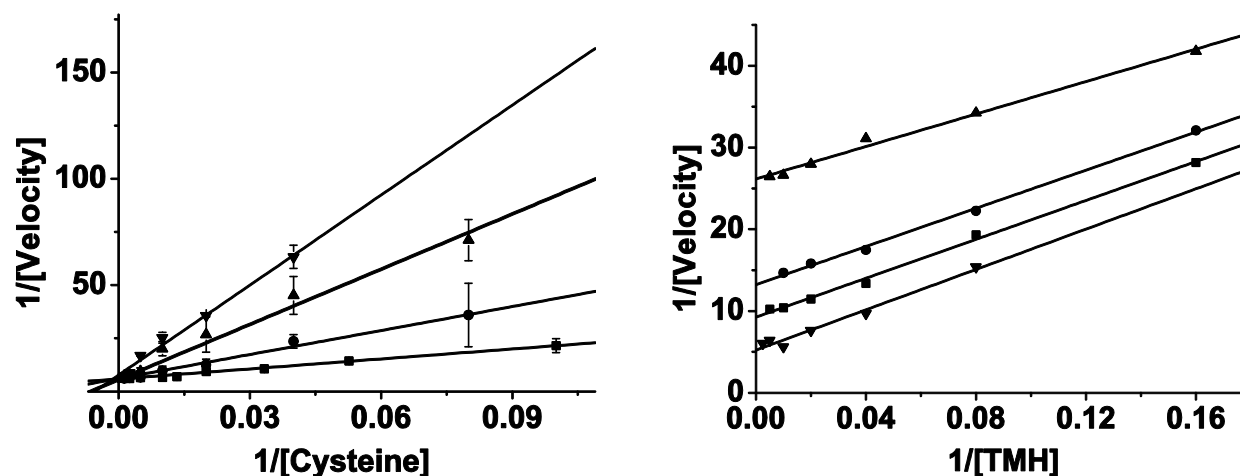


**Figure 2.** Lineweaver–Burk plots for catalytic rates recorded at 26°C in the presence of 0.2 mM TMH, variable [Cys] (left); or in the presence of 0.1 mM Cys and variable [TMH] (right). [SeCys] was kept constant at 0 mM (■), 0.05 mM (●), 0.1 mM (▲), 0.2 mM (▼). The reactions contained 100 mM HEPES buffer at pH 8.0, 100 mM NaCl, 2 mM ascorbate, 2 mM TCEP, 4  $\mu\text{M}$   $\text{FeSO}_4$ , and 1.3  $\mu\text{M}$  *CthEgtB*. The production rates of **3** were measured by HPLC. The corresponding Michaelis–Menten plots are shown in Figure S4.

**SeCys is a Cys-competitive inhibitor.** Enzyme-catalyzed C-Se bond formation may be slow because SeCys is a poor ligand for *CthEgtB*. To test this idea, we examined the ability of SeCys to inhibit turnover of Cys. First, we recorded rates of enzyme-catalyzed

formation of **3** in the presence of 0.2 mM TMH and variable concentrations of Cys and SeCys (Figure 2, Figure S4). The Lineweaver–Burk plot of the measured rates reveals that increasing the concentration of SeCys increases  $K_{M,Cys}$  but does not affect  $k_{cat}$ , suggesting that SeCys acts as a Cys-competitive inhibitor. We calculated an inhibitory constant ( $K_i$ ) for SeCys of  $17 \pm 4 \mu\text{M}$  using the following relation:

$$K_{m_{app}} = K_m \left( 1 + \frac{[I]}{K_i} \right)$$

Secondly, we determined the production rates of **3** in the presence of 0.1 mM Cys and variable concentrations of TMH (Figure 2, Figure S4). The corresponding Lineweaver–Burk plot showed that increasing the concentration of SeCys decreases both  $k_{cat}$  and  $K_{M,TMH}$ , revealing SeCys as an uncompetitive inhibitor with respect to TMH, meaning that SeCys does not bind to the enzyme in the absence of TMH. The two inhibition patterns suggest that the ternary complex (*CthEgtB*:TMH:Cys) forms through an obligatory binding sequence with TMH as the leading substrate.<sup>[15]</sup> This binding sequence is consistent with the crystal structure of *CthEgtB* in complex with TMH (PDB: 6QKJ, Figure 3). The binding sites for TMH and iron are located at the bottom of a deep tunnel. A model of the ternary complex (*CthEgtB*:TMH:Cys, Figure 3) shows that Cys binds on top of TMH and partially blocks the access to the TMH binding site (Figure 3).<sup>[6a, 6f]</sup>

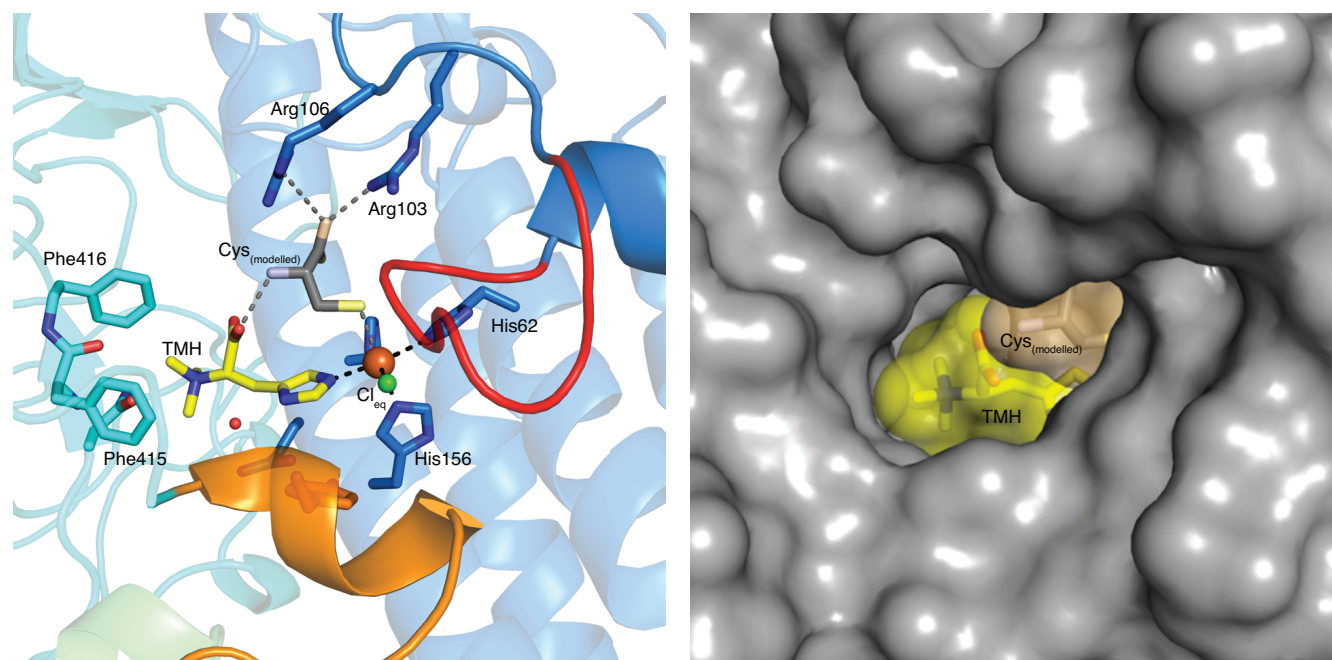
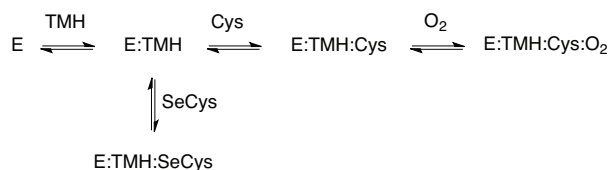


**Figure 3.** Active Site of *CthEgtB*. **Left:** Stick and cartoon representation of the active site of *CthEgtB* located between the N-terminal domain (blue) and the C-terminal domain (turquoise). Iron (II) (brown sphere) is coordinated by His62, His 152 and His 156 and the imidazole ring of TMH. The equatorial chloride ligand (green, Cl<sub>eq</sub>) indicates the position of the presumed O<sub>2</sub>-binding site. A second Cl in an axial position is not shown. Instead, Cys was modelled to bind to iron (II) through the axial coordination site.<sup>[6f]</sup> Active site loop 1 (red, residues 93-99) and active site loop 2 (orange, residues 378-386) are disordered in the native structure (PDB: 6QKI) but can fold over the active site when TMH is present (PDB: 6QKJ). **Right:** *CthEgtB* (gray surface) in complex with TMH (yellow) and Cys (brown) viewed from the active site entrance. Cys partially blocks access to the TMH binding site.

Interestingly, this binding sequence is not apparent in the absence of SeCys. Measuring the catalytic rates at variable [TMH] and constant [Cys], or constant [TMH] and variable [Cys] produced two Lineweaver–Burk plots with parallel lines (Figure S5). This pattern is typical for enzymes that catalyze two independent half-reactions in a ping-pong mechanism. However, such a mechanism is difficult to reconcile with the fact that oxidative coupling requires the simultaneous presence of Cys and TMH. More likely, the observed pattern emerges from a sequential mechanism where binding of O<sub>2</sub> to the *CthEgtB*:TMH or the *CthEgtB*:TMH:Cys complex is irreversible, for example because [O<sub>2</sub>] (0.25 mM) is saturating.<sup>[16]</sup> The kinetic behavior alone does not directly reveal as to whether O<sub>2</sub> binds before or after Cys. However, previous work on non-heme iron enzymes established that O<sub>2</sub>-binding is usually the last step in the formation of the reactive complex.<sup>[17]</sup> Indeed, the crystal structure of EgtB from *Mycobacterium thermoresistibile* (*MthEgtB*) showed that both substrates - TMH and  $\gamma$ -GCys - can bind prior to O<sub>2</sub>,<sup>[6a]</sup> suggesting that sulfoxide synthases follow a similar substrate-binding mechanism (O<sub>2</sub> last) as most non-heme iron enzymes (Scheme 1).



**Scheme 1.**

**Comparison to cysteine dioxygenase.** The observation that the SeCys-bound *CthEgtB* can hardly produce oxidation products suggests that this complex cannot efficiently activate O<sub>2</sub>. A similar observation has been made with cysteine dioxygenase (CDO). This enzyme too fails to oxidize SeCys.<sup>[18]</sup> Although CDOs are unrelated to sulfoxide synthases, their active sites are remarkably similar. Both enzymes contain an iron (II) center coordinated by a three-histidine facial triad.<sup>[6a, 6f, 19]</sup> Both enzymes coordinate their substrates directly to the metal via one sulfur and one nitrogen-ligand, reserving a sixth coordination site for O<sub>2</sub> binding. The structural similarity between the two enzyme types is also reflected by similar activity. *CthEgtB* and other sulfoxide synthases have significant thiol dioxygenase activity.<sup>[6e, 6f, 20]</sup> Spectroscopic characterization showed that CDO binds SeCys in the same way as Cys, but that the CDO:SeCys complex is entirely unreactive with O<sub>2</sub>. Computational models confirmed that the S-to-Se substitution dramatically reduces the ability of the iron (II) center to bind O<sub>2</sub>.<sup>[18b]</sup> The catalytic activity of *CthEgtB* towards SeCys might be affected by the same problem. On the other hand, since this limitation is not fundamental it is conceivable that sulfoxide synthases with slightly different active sites might indeed catalyze C-Se bond formation more efficiently.

**Comparison with other sulfoxide synthases.** With this thought in mind we examined the C-Se bond forming activities of other sulfoxide synthases. Bacterial and eukaryotic homologs with known activities can be classified into four types distinguished by significant differences in their active site geometries and their substrate preferences.<sup>[6f]</sup> Briefly, *CthEgtB* represents type II sulfoxide

synthases. Type I EgtBs such as *MthEgtB* consume  $\gamma$ -GCys instead of Cys as the sulfur donor.<sup>[6a]</sup> Type III enzymes are fungal sulfoxide synthases that use Cys as the sulfur donor.<sup>[21]</sup> In our study, type III enzymes are represented by the sulfoxide synthase from the thermophilic filamentous fungus *Chaetomium thermophilum* (*CthEgt1*, Type III). Most type IV sulfoxide synthases, such as *OvoA* from *Erwinia tasmaniensis* (*EtaOvoA*), produce sulfoxide **11** as a biosynthetic intermediate of ovothiol (**12**, Figure 1).<sup>[22]</sup> However, when presented with TMH as a sulfur acceptor *EtaOvoA* can also produce the same product as type II and III enzymes (sulfoxide **3**).<sup>[23]</sup> In fact, cyanobacterial *OvoA* homologs have adapted to produce sulfoxide **3** which further underscores the functional and mechanistic similarity between type IV and I – III enzymes.<sup>[24]</sup> The C-S and C-Se bond forming abilities of these representative type I – IV sulfoxide synthases were assayed in reactions containing 1 mM TMH and 1 mM Cys or SeCys. The activity of *MthEgtB* was assayed using  $\gamma$ -GCys or  $\gamma$ -glutamyl selenocysteine ( $\gamma$ -GSeCys) as the second substrate (Table 1). This comparison showed that the bacterial enzymes catalyze TMH selenation about two orders of magnitude slower than sulfurization (Table 2). In contrast, the fungal enzyme *CthEgt1* produced selenoether **4** almost as fast as sulfoxide **3**. Because of the robust activity we could determine the Michaelis-Menten parameters for *CthEgt1*-catalyzed formation of selenoether **4** and sulfoxide **3** ( $k_{\text{cat,Cys}} = 0.07 \pm 0.01$ ;  $K_{\text{M,Cys}} = 38 \pm 3$  uM;  $k_{\text{cat,SeCys}} = 0.04 \pm 0.01$ ;  $K_{\text{M,SeCys}} = 33 \pm 6$  uM, Figure S6). These parameters show that *CthEgt1* accepts SeCys and Cys with very similar efficiency.

The difference in S vs. Se selectivities between bacterial and fungal enzymes is interesting for two reasons. First, these observations suggest that either only fungi can produce **2**, or that this oranoselenide emerges from an entirely different biosynthetic process. The similar catalytic parameters associated with *CthEgt1*-catalyzed production of **3** and **4** suggest that the production rates of **1** and **2** *in vivo* may be directly related to the cellular concentrations of Cys and SeCys. In most organisms the concentration of SeCys is kept very low to avoid oxidative stress and inadvertent incorporation in place of Cys during ribosomal protein synthesis.<sup>[25]</sup> In fact, specific ribosomal insertion of SeCys into selenoproteins usually depends on sophisticated co-translational systems that do not require free SeCys as a substrate.<sup>[26]</sup> Hence, free SeCys appears as an unlikely building block for specific biosynthesis of selenometabolites. Since Cys-biosynthetic enzymes cannot efficiently distinguish between sulfur and selenium,<sup>[27]</sup> high concentrations of selenium in the environment can increase the concentration of SeCys relative to that of Cys.<sup>[7b, 27]</sup> Therefore, production of selenoneine by *S. pombe* may simply be a unspecific response to high selenium concentrations in the growth medium.<sup>[8]</sup> The physiological relevance of this unspecific response is unclear. If certain organisms do produce selenoneine as a specific metabolite with a specific purpose, they are likely to use a different set of enzymes than for ergothioneine biosynthesis and a selenium-donor that is less problematic than SeCys.



Secondly, our observations identify fungal sulfoxide synthases as interesting targets for protein crystallography. Since *CthEgtB* and *CthEgt1* both bind SeCys efficiently, the catalytic differences between the two enzymes must lie in the O<sub>2</sub> binding pocket. Apparently, fungal enzymes bind and activate O<sub>2</sub> in a way that is largely insensitive to the S-to-Se substitution. Comparison between the active sites of fungal and bacterial enzymes will be important to identify the structural determinants for these different behaviour. Unfortunately, the sequence alignment of *CthEgt1* and the two crystallized homologs *CthEgtB* and *MthEgtB* shows that the protein segment participating in Cys- and O<sub>2</sub>-binding is highly variable, precluding the construction of a reliable homology model of fungal enzymes (Figure S7).<sup>[6a, 6f]</sup> Hence, a search for structural differences that enable C-Se bond formation can only begin once a crystal structure of type III sulfoxide synthases becomes available.

**Table 1.** Comparison between C-S and C-Se bond formation activity of type I – IV sulfoxide synthases.<sup>[a]</sup>

enzyme	type	$k_{\text{obs,S}}$ [s <sup>-1</sup> ]	$k_{\text{obs,Se}}$ [s <sup>-1</sup> ]	$k_{\text{obs,S}}/k_{\text{obs,Se}}$	$^{\text{D}}V_{\text{app,S}} / ^{\text{D}}V_{\text{app,Se}}$
<i>MthEgtB</i>	I	0.75	0.012	60	n.d.
<i>CthEgtB</i>	II	0.2	0.0012	170	$0.9 \pm 0.1/3.1 \pm 0.1$
<i>CthEgt1</i>	III	0.07	0.04	2	$1.0 \pm 0.1/1.2 \pm 0.1$
<i>EtaOvoA</i>	IV	0.03	0.00007	470	n.d.

<sup>[a]</sup> Reaction conditions: 100 mM phosphate buffer pH 8.0, 100 mM NaCl, 2 mM ascorbate, 2 mM TCEP, 4 μM FeSO<sub>4</sub>, 0.5 mM TMH, 0.5 mM γGSeCys or 0.5 mM SeCys, 26°C.

**SeCys as a mechanistic probe.** *CthEgtB* and *CthEgt1* differ by one more aspect that might provide new insight into the catalytic mechanism of sulfoxide synthases. The slow production of selenoether **4** by *CthEgtB* is subject to a large substrate kinetic isotope effect of  $3.1 \pm 0.1$  (Table 1, Figure S8). This effect is an observed kinetic isotope effect ( $^{\text{D}}V_{\text{app,SeCys}}$ )<sup>[28]</sup> determined by comparing the production rate of **4** in reactions containing saturating concentrations of SeCys (0.5 mM) and TMH (0.5 mM) or C<sub>2</sub>-<sup>2</sup>H-TMH, the isotopolog of TMH deuterated at C<sub>2</sub> of the imidazole ring. An isotope effect of this magnitude is attributable to a primary isotope effect – related to C-H bond cleavage. Secondary isotope effects and binding isotope effects are usually much smaller.<sup>[6e, 29]</sup> In contrast, the Cys-containing reaction is characterized by a substrate isotope effect near unity ( $^{\text{D}}V_{\text{app,Cys}} = 0.9 \pm 0.1$ , Table 1, Figure S8). Similar experiments with *MthEgtB*<sup>[20b]</sup> (γGCys) and *EtaOvoA* (Cys),<sup>[6e, 30]</sup> produced kinetic isotope effects near unity, suggesting that C-H cleavage generally has little effect on the overall rate of the native reactions. Interestingly, *CthEgt1*-catalyzed consumption of C<sub>2</sub>-<sup>2</sup>H-TMH/TMH is also characterized by an isotope effects near unity with either Cys or SeCys as substrates (Table 1, Figure S9).

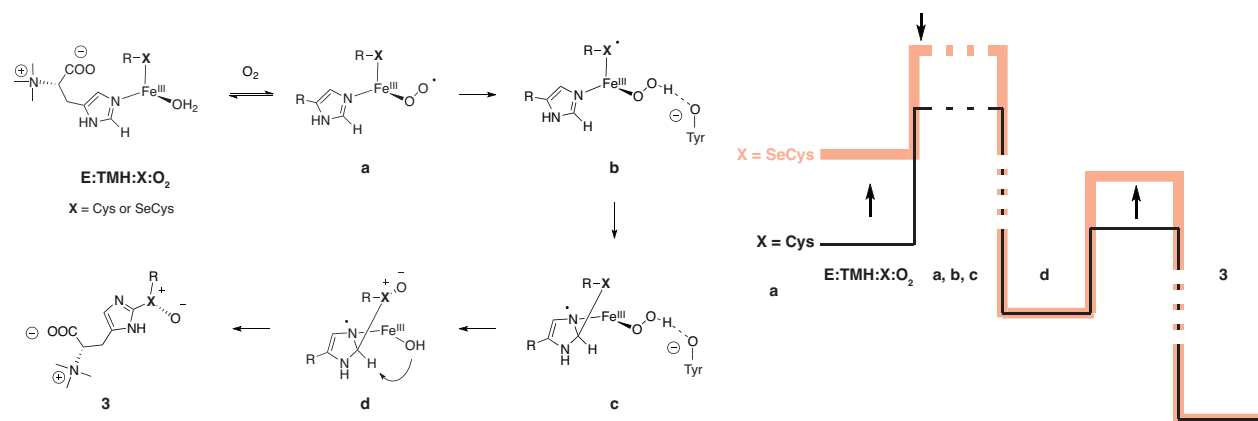


**Figure 4.** Left: Proposed mechanism for sulfoxide synthase-catalyzed oxidative coupling of TMH to Cys or SeCys. Right: Qualitative potential-energy landscape for this reaction with Cys (black) or SeCys (orange) as substrate. Black arrows indicate suggested changes in the potential-energy landscape effected by the S to Se substitution.

The large isotope effect for *CthEgtB*-catalyzed turnover of SeCys is the first probe available to directly examine C-H bond cleavage, and provides qualitative information about the energy landscape of the entire reaction coordinate. Four potential mechanisms for this complicated reaction have been proposed. Three mechanisms for the sulfoxide synthase reaction have been proposed based on computation. These models provide valuable estimations of barrier highs associated with elementary steps.<sup>[6b-d]</sup> However, as we have discussed elsewhere,<sup>[6f]</sup> these models are not consistent with all observables, such as the stereochemistry of the product, and predict isotope effects that are not observed. Therefore we base the following discussion on a fourth mechanism which has not yet been examined by computation, but has so far survived all experimental scrutiny (Figure 4). In this mechanism the iron-bound superoxide in the reactive complex (**a**) is protonated by Tyr93 (*CthEgtB*) or Tyr377 (*MthEgtB*) and reduced by the iron-coordinated Cys (or  $\gamma$ GCys). The resulting species **b** reacts to **c** via C-S bond formation, followed immediately by oxidation of the sulfur atom (S-O bond formation). Proton abstraction from carbon 2 (**e**) produces the rearomatized product sulfoxide **3**. This mechanism can be segmented into three phases: i) Formation of the reactive complex (E:TMH:Cys:O<sub>2</sub>), ii) C-S and/or S-O bond formation, and c) C-H bond cleavage. To examine as to why the S-to-Se substitution increases the observed kinetic isotope effect on C-H cleavage for *CthEgtB* but not for *CthEgt1* we need to consider the possible effects of this substitution on each of these three reaction phases. The expression of an intrinsic kinetic isotope effect (<sup>D</sup>k<sub>C-H</sub>) on the observed isotope effect (<sup>D</sup>V) is influenced by three kinetic functions:<sup>[31]</sup> i) a function termed *forward ratio of catalysis* (*R<sub>f</sub>*), comparing the barrier height of the isotope-sensitive step forward with those of the remaining forward steps; ii) the *reverse commitment to catalysis* (*C<sub>f</sub>*), describing the extent to which the isotope sensitive step is equilibrating; and iii) a function that encompasses all equilibria that link formation of the enzyme:substrate complex with the isotope sensitive step (*forward equilibration preceding catalysis*, *E<sub>f</sub>*). These functions relate <sup>D</sup>V and <sup>D</sup>k<sub>C-H</sub> as follows:

$$^D V = (^D k_{C-H} + R_f / E_f + C_f \times K_{eq}) / (1 + R_f / E_f + C_f)$$

This comprehensive relation simplifies if the reaction includes irreversible steps: C-H cleavage (**d** → **3**, Figure 4) is coupled to irreversible aromatization of the imidazole ring.<sup>[6b, 6c]</sup> Irreversibility of this step reduces  $C_f$  to zero. S-O bond formation (**c** → **d**) is also a strongly exothermic reaction, and most likely irreversible. Under these conditions  $E_f$  approaches unity.<sup>[6c]</sup> Hence, the relation simplifies to

$$^D V = (^D k_{C-H} + R_f) / (1 + R_f)$$

meaning that the expression of the intrinsic isotope effect likely depends on the forward net rate constants across the preceding or succeeding steps.<sup>[32]</sup> Perturbations that slow down steps other than the isotope sensitive step would *decrease* the expression of  $^D k_{C-H}$  on the observed rate. As discussed above, the S-to-Se substitution reduces the O<sub>2</sub> activation efficiency of *CthEgtB* by at least 10 and more likely 100-fold. Making O<sub>2</sub> activation more difficult should – if anything – *decrease* the expression of  $^D k_{C-H}$  on the maximal velocity. Since the S-to-Se substitution *increases* the expression of  $^D k_{C-H}$  for *CthEgtB* we conclude that O<sub>2</sub> activation is not the only affected step.

In addition, C-H bond cleavage (**d** → **3**) may become more difficult. Indeed, there is published evidence that protons  $\alpha$  to selenoethers can be less acidic than protons  $\alpha$  to thioethers.<sup>[33]</sup> Less is known about protons  $\alpha$  to selenoxides or sulfoxides. As a model reaction we compared the rates of proton to deuterium exchange (H/D exchange) at the methyl groups of dimethylsulfoxide (DMSO) and dimethylselenoxide (DMSeO, Figure S10). In reactions containing deuterium oxide as solvent and tetramethylammonium hydroxide as base incubated at 60°C we observed 4-fold faster H/D exchange in DMSO than in DMSeO. Hence the S-to-Se substitution can indeed slow down C-H cleavage (**d** → **3**). However, since the rate of O<sub>2</sub> activation is reduced by at least 10, the reduction of the rate for C-H cleavage would have to be much larger in order to increase the observable isotope effect. On the other hand, a dramatic increase of the intrinsic barrier height associated with C-H cleavage is inconsistent with the observation that *CthEgt1*-catalyzed turnover of SeCys and Cys occur at similar rates, and with the same isotope effects near unity.

The most convincing explanation for the observed isotope effects is that the S-to-Se substitution accelerates chemical steps preceding C-H cleavage. Indeed, organoselenides are usually characterized with a lower redox potential and higher polarizability than their

sulfur isologs.<sup>[3d, 34]</sup> This increased reactivity could lower the reaction barriers for oxidation (**b** → **c**), C-Se bond formation (**c** → **d**) and oxygen transfer to Se (**d** → **e**). A qualitative energy landscape drawn for the Cys- and SeCys-containing reactions illustrates how reduction of these barriers could increase the expression of the intrinsic substrate kinetic isotope effect on the observed rate of the SeCys reaction (Figure 5). Increase of the barrier associated with C-H cleavage (as discussed above) would influence the isotope effect in the same direction.

In this interpretation, the reactive complex with selenium (**b**) appears as a more reactive species with regard to the forward reaction than the same complex with sulfur. Therefore, we suggest that careful characterization of the geometric and electronic structures of these two species by computational methods could help to identify the precise basis for the increased reactivity, and the precise nature of the reaction forward. The active site of *CthEgt1* appears to mitigate the chemical differences between the sulfur and selenium versions of **b**. Characterization of the substrate binding pockets of this enzyme by high-resolution crystallography is therefore another important objective en route to understanding the catalytic mechanism of sulfoxide synthases.

## Conclusions

In this report we described the catalytic activity of bacterial and fungal sulfoxide synthases with selenol instead of thiol substrates. Bacterial enzymes catalyze oxidative coupling of TMH to SeCys or  $\gamma$ GSeCys two orders of magnitude less efficiently than coupling to Cys or  $\gamma$ GCys. Based on these observations we conclude that bacteria are not likely to produce selenoneine (**2**) from SeCys in a sulfoxide synthase-dependent reaction. The substrate-binding mechanism, the inhibitory activity of SeCys and the slow turnover of SeCys observed for *CthEgtB* provide evidence that the S-to-Se substitution reduces the ability of the enzyme:substrate complex to bind and/or activate O<sub>2</sub>. The contrasting behavior of *CthEgt1* points to significant differences in the O<sub>2</sub>-binding mechanism between fungal and bacterial enzymes. Furthermore, we described a mechanistic interpretation of the observed substrate kinetic isotope effects suggesting that the S-to-Se substitution affects more than one elementary step along the reaction coordinate. We hope that these findings inspire additional empirical and computational enquiries into the nature of this complicated enzyme reaction.

## ACKNOWLEDGMENT

K.V.G is a recipient of a Swiss Government Fellowship for Excellence; C.L. is a recipient of a SSSTC & CSC postdoctoral fellowship; F.P.S. is supported by the “Professur für Molekulare Bionik” and by a starting grant from the European Research Council (ERC-2013- StG 336559).

## REFERENCES

- [1] aK. D. Asmus, R. V. Bensasson, J. L. Bernier, R. Houssin, E. J. Land, *Biochem. J.* **1996**, *315*, 625-629; bC. Stoffels, M. Oumari, A. Perrou, A. Termath, W. Schlundt, H. G. Schmalz, M. Schäfer, V. Wewer, S. Metzger, E. Schömig, D. Gründemann, *Free Radic Biol Med.* **2017**, *113*, 385 - 394; cB. Halliwell, I. K. Cheah, R. M. Y. Tang, *FEBS Lett.* **2018**, *592*, 3357 - 3366; dL. Servillo, N. D'Onofrio, M. L. Balestrieri, *J Cardiovasc Pharmacol.* **2017**, *69*, 183 - 191.
- [2] aY. Yamashita, M. Yamashita, *J. Biol. Chem.* **2010**, *285*, 18134-18138; bY. Yamashita, M. Yamashita, H. Iida, *Nutrients* **2013**, *5*, 388 - 395.
- [3] aM. Yamashita, Y. Yamashita, T. Ando, J. Wakamiya, S. Akiba, *Biol. Trace. Elem. Res.* **2013**, *156*, 36 - 44; bM. P. Rayman, *Lancet* **2012**, *379*, 1256 - 1268; cJ. Masuda, C. Umemura, M. Yokozawa, K. Yamauchi, T. Seko, M. Yamashita, Y. Yamashita, *Nutrients* **2018**, *10*, E1380; dA. S. Rahmanto, M. J. Davies, *IUBMB Life* **2012**, *64*, 863 - 871.
- [4] aB. M. Cumming, K. C. Chinta, V. P. Reddy, A. J. C. Steyn, *Antioxid. Redox Signal.* **2018**, *28*, 431 - 444; bH. S. Saini, B. M. Cumming, L. Guidry, D. A. Lamprecht, J. H. Adamson, V. P. Reddy, K. C. Chinta, J. H. Mazorodze, J. N. Glasgow, M. Richard-Greenblatt, A. Gomez-Velasco, H. Bach, Y. Av-Gay, H. Eoh, K. Rhee, A. J. C. Steyn, *Cell Rep.* **2016**, *14*, 572 - 585.
- [5] aA. Askari, D. B. Melville, *J. Biol. Chem.* **1962**, *237*, 1615-&; bF. P. Seebeck, *J. Am. Chem. Soc.* **2010**, *132*, 6632-6633.
- [6] aK. V. Goncharenko, A. Vit, W. Blankenfeldt, F. P. Seebeck, *Angew. Chem. Int. Ed. Engl.* **2015**, *54*, 2821 - 2824; bW. J. Wei, P. E. Siegbahn, R. Z. Liao, *Inorg. Chem.* **2017**, *56*, 3589 - 3599; cA. S. Faponle, F. P. Seebeck, S. P. de Visser, *J. Am. Chem. Soc.* **2017**, *139*, 9259 - 9270; dG. Tian, H. Su, Y. Liu, *ACS Catalysis* **2018**, *8*, 5875 - 5889; eL. Chen, N. Naowarojna, H. Song, S. Wang, J. Wang, Z. Deng, C. Zhao, L. P., *J. Am. Chem. Soc.* **2018**, *140*, 4604 - 4612; fA. Stampfli, K. V. Goncharenko, M. Meury, B. Dubey, T. Schirmer, F. P. Seebeck, *J Am Chem Soc* **2019**, *141*, 5275 - 5285.
- [7] aT. C. Stadtman, *Annu Rev Biochem.* **1990**, *59*, 111 - 127; bC. Arnaudguilhem, K. Bierla, L. Ouerdane, H. Preud'homme, A. Yiannikouris, R. Lobinski, *Anal Chim Acta.* **2012**, *757*, 26 - 38.
- [8] aT. Pluskal, M. Ueno, M. Yanagida, *PLoS One* **2014**, *9*, e97774; bN. G. Turrini, N. Kroepfl, K. B. Jensen, T. C. Reiter, K. A. Francesconi, T. Schwerdtle, W. Kroutil, D. Kuehnelt, *Metallomics* **2018**, *10*, 1532 - 1538.
- [9] aI. Rohn, N. Kroepfl, M. Aschner, J. Bornhorst, D. Kuehnelt, T. Schwerdtle, *J Trace Elem Med Biol.* **2019**, *55*, 78 - 81; bI. Rohn, N. Kroepfl, J. Bornhorst, D. Kuehnelt, T. Schwerdtle, *Mol Nutr Food Res.* **2019**, *63*, e1900080; cR. Alhasan, M. J. Nasim, C. Jacob, c. Gaucher, *Curr Pharmacol Rep* **2019**, *5*, 163 - 173.
- [10] D. Lim, D. Gründemann, F. P. Seebeck, *Angew Chem Int Ed Engl* **2019**, *in press*.
- [11] H. Song, W. Hu, N. Naowarojna, A. S. Her, S. Wang, R. Desai, L. Qin, X. Chen, P. Liu, *Sci Rep.* **2015**, *5*, 11870.
- [12] A. M. Gamage, C. Liao, I. K. Cheah, Y. Chen, D. R. X. Lim, J. W. K. Ku, R. S. L. Chee, M. Gengenbacher, F. P. Seebeck, B. Halliwell, Y. H. Gan, *FASEB, J* **2018**, *11*:ff201800716.
- [13] S. Dery, P. S. Reddy, L. Dery, R. Mousa, R. N. Dardashti, N. Metanis, *Chem. Sci.* **2015**, *6*, 6207 - 6212.
- [14] aH. J. Reich, R. J. Hondal, *ACS Chem Biol.* **2016**, *11*, 821 841; bV. De Silva, M. M. Woznichak, K. L. Burns, K. B. Grant, S. W. May, *J. Am. Chem. Soc.* **2004**, *126*, 2409 - 2413.
- [15] aH. J. Fromm, V. Zewe, *J. Biol. Chem.* **1962**, *237*, 3027 - 3032; bD. L. Purich, *Enzyme Kinetics*, Academic Press, London, **2010**.
- [16] H. J. Fromm, *Biochim. Biophys. Acta* **1967**, *39*, 221 - 230.
- [17] E. I. Solomon, S. Goudarzi, K. D. Sutherlin, *Biochemistry* **2016**, *55*, 6363 - 6374.
- [18] aJ. D. Gardner, B. S. Pierce, B. G. Fox, T. C. Brunold, *Biochemistry* **2010**, *49*, 6033-6041; bE. Blaesi, J. D. Gardner, B. G. Fox, T. C. Brunold, *Biochemistry* **2013**, *52*, 6040 - 6051.
- [19] C. A. Joseph, M. J. Maroney, *Chem. Commun.* **2007**, 3338-3349.
- [20] aH. Song, A. S. Her, F. Raso, Z. Zheng, Y. Huo, P. Liu, *Org. Lett.* **2014**, *16*, 2122-2125; bK. V. Goncharenko, F. P. Seebeck, *Chem. Commun.* **2016**, *52*, 1945 - 1948.
- [21] aK. J. Sheridan, B. E. Lechner, G. O. Keeffe, M. A. Keller, E. R. Werner, H. Lindner, G. W. Jones, H. Haas, S. Doyle, *Sci Rep.*

- 2016**, *6*, 35306; bW. Hu, H. Song, A. Sae Her, D. W. Bak, N. Naowarojna, S. J. Elliot, L. Qin, X. Chen, P. Liu, *Org. Lett.* **2014**, *16*, 5382 - 5385; cM. H. Bello, V. Barrera-Perez, D. Morin, L. Epstein, *Fungal Genet. Biol.* **2012**, *49*, 160-172.
- [22] aA. Braunshausen, F. P. Seebeck, *J. Am. Chem. Soc.* **2011**, *133*, 1757-1759; bI. Castellano, F. P. Seebeck, *Nat. Prod. Rep.* **2018**, *35*, 1241 - 1250; cN. Naowarojna, R. Cheng, L. Chen, M. Quill, M. Xu, C. Zhao, P. Liu, *Biochemistry* **2018**, *57*, 3309 - 3325.
- [23] H. Song, M. Leninger, N. Lee, P. Liu, *Org. Lett.* **2013**, *15*, 4854 - 4857.
- [24] C. Liao, F. P. Seebeck, *ChemBioChem* **2017**, *18*, 2115 - 2118.
- [25] aJ. Lu, A. Holmgren, *J. Biol. Chem.* **2009**, *284*, 723 - 727; bM. Lazard, M. Dauplais, S. Blanquet, P. Plateau, *Biomol Concepts* **2017**, *8*, 93 - 104; cS. Wang, A. T. Al-Soodani, G. C. Thomas, B. A. Buck-Koehntop, K. J. Woycechowsky, *Bioconj. Chem.* **2018**, *29*, 2332 - 2342.
- [26] V. M. Labunsky, D. L. Hatfield, V. N. Gladyshev, *Physiol Rev.* **2014**, *94*, 739 - 777.
- [27] M. Birringer, S. Pilawa, L. Flohé, *Nat Prod Rep.* **2002**, *19*, 693 - 718.
- [28] D. B. Northrop, *Annu Rev Biochem.* **1981**, *50*, 103 - 131.
- [29] aR. A. Caldwell, H. Misawa, *J. Am. Chem. Soc.* **1987**, *109*, 6869 - 6870; bK. W. Rickert, J. P. Klinman, *Biochemistry* **1999**, *38*, 12218 - 12228.
- [30] G. T. Mashabela, F. P. Seebeck, *Chem. Commun.* **2013**, *49*, 7714 - 7716.
- [31] D. B. Northrop, *Biochemistry* **1981**, *20*, 4056 - 4061.
- [32] W. W. Cleland, *Biochemistry* **1975**, *14*, 3220 - 3224.
- [33] H. J. REICH, W. W. WILLIS, *J. Org. Chem.* **1980**, *45*, 5227 - 5229.
- [34] aR. J. Hondal, S. M. Marino, V. N. Gladyshev, *Antiox. Redox Signal.* **2013**, *18*, 1675 - 1689; bC. Jacob, G. I. Giles, N. M. Giles, H. Sies, *Angew Chem Int Ed Engl* **2003**, *42*, 4742 - 4758.